Int. J. Electrochem. Sci., 14 **(2019)** 4327 – 4337, doi: 10.20964/2019.05.68

International Journal of
ELECTROCHEMICAL
SCIENCE
www.electrochemsci.org

A Novel Electrochemical Sensor Based on the Synergistic Effect of Trace Platinum and Foliate $Co_{0.85}Se$ for the Determination of Dopamine

Xiang Li[1,2], *Miaomiao Chen*[1,2], *Rong Rui*[1], *Zhigui Wan*[1], *Feng Chen*[1], *Xiaoshuang Zuo*[1], *Chang Wang*[1*], *Hai Wu*[1,2*]

[1] School of Chemistry and Materials Engineering, FuyangNormalUniversity, Fuyang, Anhui 236037, PR China
[2] Anhui Province Key Laboratory of Environmental Hormone and Reproduction, Anhui Provincial Key Laboratory for Degradation and Monitoring of Pollution of the Environment, Fuyang Normal University. Fuyang, Anhui 236037, PR China.
[*]E-mail: bigceleron@163.com; wuhai317@126.com

Received: 12 January 2019 / *Accepted:* 19 March 2019 / *Published:* 10 April 2019

Foliate cobalt selenide ($Co_{0.85}Se$) was synthesized by the hydrothermal method and was combined with trace platinum (Pt) to form a Pt/$Co_{0.85}Se$ material, which was modified on the surface of a glassy carbon electrode (GCE) to fabricate a novel nonenzymatic electrochemical sensor (Pt/$Co_{0.85}Se$/GCE) for the selective determination of dopamine (DA). On the Pt/$Co_{0.85}Se$ interface, well-separated oxidation peaks of DA, ascorbic acid (AA), and uric acid (UA) were observed due to the superior conductivity of $Co_{0.85}Se$ and the excellent catalytic activity of Pt. With the synergistic effect of Pt and $Co_{0.85}Se$, the linear range for DA detection was found to be 0.50–22.0 μM with a detection limit of 0.39 μM (S/N=3) and a high sensitivity of 2306 μA mM^{-1} cm^{-2}. Furthermore, the proposed sensor exhibited high selectivity for the determination of DA in the presence of UA, AA, and other potential interferences, which indicated that the sensor showed great potential for practical and reliable DA analysis of serum samples.

Keywords: Electrochemical sensor, Cobalt selenide, Dopamine, Platinum

1. INTRODUCTION

Dopamine (DA), as a natural neurotransmitter, is responsible for the regulation of myriad physical and cognitive functionalities. It plays important roles in the control of central nervous system and has cardiovascular, renal, and hormonal functions. Addiyionally, it is involved in drug addiction and diseases [1,2]. Low levels of DA may induce neurological disorders such as schizophrenia and

Parkinson's disease [3]. Therefore, the development of methods for the simple, accurate, rapid, inexpensive, and selective determination of DA is highly desirable in diagnostic research [1,4].

Multifarious methods including spectroscopic [5,6], chromatographic [7], enzymatic [8], and electroanalytical methods have been explored because of their high efficiency and small sample-size requirements [9–11]. Specifically, the electrochemical technique is attractive due to its simplicity, high sensitivity, fast response, low cost, and ease of miniaturization [12]. Nonenzymatic electrochemical sensors are ideal systems for the direct oxidation or reduction of analytes and do not require fragile enzymes. We constructed several nonenzymatic electrochemical sensors to determine hydrogen peroxide, nitrite, and AA, which have several advantages including high sensitivity, selectivity, and stability [13–15]. However, for detecting DA, conventional electrodes cannot be used because it always coexists with ascorbic acid (AA) or uric acid (UA) in biological samples, which usually foul the electrodes and have oxidation potentials that greatly overlap with taht of DA [16,17]. Thus, these harsh requirements motivate major efforts for developing stable, sensitive, and selective interfacial materials for detecting DA.

Many nanomaterials, including carbon nanomaterials, inorganic or organic compounds, and noble metal nanoparticles (NPs) [18–20], have been used for constructing electrochemical sensors because of their unique catalytic and electrochemical activities. Platinum (Pt) NPs have been of particular interest due to their roles in many catalytic reactions and the controllable specific surfaces of electrodes [21]. Xu et al. chemically reduced Pt NPs on reduced graphene oxide for the detection of DA and UA in the presence of AA, which showed high selectivity [9]. Thiagarajan et al. proposed a biosensor based on electrochemical deposition of Pt and gold (Au) NPs with L-cysteine on a glassy carbon electrode (GCE), and achieved the simultaneous determination of AA, DA, and UA [22]. Therefore, Pt is excellent electrode materials for fabricating electrochemical sensors. However, the scarcity and high cost of the noble metal Pt limit its wide application. Alternative nanocomposites containing trace Pt have the synergistic effects of Pt and support materials, such as graphene [9,23], carbon nanotubes [24], and metallic hybrid [25], which can reduce the consumption of Pt and improve catalytic ability.

Metal chalcogenides, including metal sulfides and selenides are considered to be perfect alternatives for use as electrode materials due to their high conductivity and excellent catalytic activity [26]. Specifically, transition-metal selenides have been extensively applied in the fields of rechargeable batteries, supercapacitors, and catalysts [27]. Among them, cobalt selenides (CoSe) have exhibited good performance in energy storage devices [28], as counter-electrodes in dye-sensitized solar cells (DSSCs) [29], and in catalysis [30]. However, CoSe have been scarcely used as electrode materials to construct nonenzymatic electrochemical sensors for applications in the field of analytical chemistry.

Therefore, to take full advantages of the catalytic activity of Pt, the electrochemical properties of CoSe, and the synergistic effects thereof, graphene-like $Co_{0.85}Se$ was synthesized by the hydrothermal method and was combined with trace Pt to prepare Pt/$Co_{0.85}Se$ nanocomposites. The as-prepared Pt/$Co_{0.85}Se$ nanocomposites were used as electrode materials to fabricate a novel nonenzymatic electrochemical sensor. To evaluate the performance of the sensor, DA was used as the model target to investigate the catalytic activity and selectivity of the sensor. The results suggest that

the sensor has several advantages as follows: a very small amount of Pt was employed; the electrochemically active area was enlarged; the electrocatalytic activity, sensitivity and selectivity for the determination of DA were improved, and the sensing behavior in blood serum samples was attractive. We anticipate that the proposed method can extend the application range of CoSe material in analytical chemistry and can provide a new strategy to construct novel electrochemical sensors.

2. EXPERIMENTAL

2.1. Reagents and chemicals

Se powder (99.999%), $CoCl_2·6H_2O$ (99.9%, Aladdin), and $N_2H_4·H_2O$ (85 wt %) were purchased from Aladdin (Shanghai, China). Chloroplatinic acid hexahydrate ($H_2PtCl_6·6H_2O$, 99.9%) was bought from Sinopharm Chemical Reagent *Co., Ltd.* (Shanghai, China). Phosphate buffered saline solution (PBS, 0.10 M, containing 0.10 M KCl) with different pH was measured with a pH meter (Mettler, Toledo, Canada). The serum sample was centrifuged at 4000 rpm at 4 °C for 20 min, and it was then diluted to the desirable concentrations with 0.01 M PBS.

2.2. Synthesis of $Co_{0.85}Se$

Cobalt selenides ($Co_{0.85}Se$) was synthesized *via* a one-step hydrothermal reaction. Briefly, 0.12 mmol Se powder and 0.1 mmol $CoCl_2·6H_2O$ were dissolved in 25.0 mL ultrapure water, and then 7.5 mL $N_2H_4·H_2O$ was added under sonication for 20 min. Subsequently, 6.5 mL mixed solution was placed into a 10 mL Teflon-lined autoclave while stirred for 7 minutes. The autoclave was tightly sealed and heated at 120 °C for 12 h and was then cooled to room temperature naturally. Black precipitate was collected and alternately washed with ethanol and ultrapure water for several cycles followed by drying under a vacuum at 80 °C for 3 h. $Co_{0.85}Se$ was then obtained for characterizing and constructing electrochemical sensor.

2.3. Preparation of modified electrodes

3.6 mg $Co_{0.85}Se$ powder was dissolved in 2.5 mL ethanol and water solution (volume ration, 1:1) by sonication for 30 min. A glassy carbon electrode (GCE) was cleaned and 10.0 μL $Co_{0.85}Se$ suspension was then dropped on its surface. It was then dried under ambient temperature to prepare $Co_{0.85}Se$/GCE. Then, 4.0 μL 4.69 mM H_2PtCl_6 aqueous solution was dropped on the surface of $Co_{0.85}Se$/GCE. After it was dried in a dark place, the modified electrode was electrochemically reduced by successive scans in 0.5 M H_2SO_4 for 25-cycles between 0.55 and −0.2 V to obtain Pt/$Co_{0.85}Se$/GCE. For comparison, $Co_{0.85}Se$/GCE was prepared using 10.0 μL $Co_{0.85}Se$ suspension and Pt/GCE was obtained by redcution of 4.0 μL H_2PtCl_6 aqueous solution in the same method.

2.4. Apparatus and measurements

Cyclic voltammetry (CV), differential pulse voltammetry (DPV), electrochemical impedance spectroscopy (EIS), and amperometric current–time (*i*–*t*) curve generation were carried out on a CHI660C electrochemical workstation (Shanghai Chenhua Co., Ltd., China). Three-electrode system consist of a fabricated sensor (Pt/$Co_{0.85}Se$/GCE), Pt wire counter electrode, and Ag/AgCl reference electrode. All the potentials in this research were reported *versus* the Ag/AgCl reference electrode. The solution in electrochemical expreiments were deoxidized by pure nitrogen for 15 min.

a Sirion 200 scanning electron microscope (SEM) equipped with energy-dispersion spectroscopy (EDS) (Netherlands) was utilized to characterize the modified electrodes and measure the elemental concentrations in the samples. X-ray diffraction (XRD) profiles of the obtained $Co_{0.85}Se$ were recorded on an X-ray powder diffractometer (X' Pert PRO, Philips) with Cu Kα radiation (λ = 0.154 nm). The composition of selenide was detected by inductively coupled plasma–atomic emission spectroscopy (ICP-AES, Thermo Jarrell Ash Corp., USA). The mass of Pt on the surface of the Pt/$Co_{0.85}Se$-modified electrode was quantified by ICP-AES. For ICP-AES analyses, the Pt/$Co_{0.85}Se$/GCE was soaked in 3.00 mL aqua regia and was sonicated for 10 min, and was then diluted to the concentration of the detecting solution.

3. RESULTS AND DISCUSSION

3.1. Characterization of $Co_{0.85}Se$ and Pt/$Co_{0.85}Se$

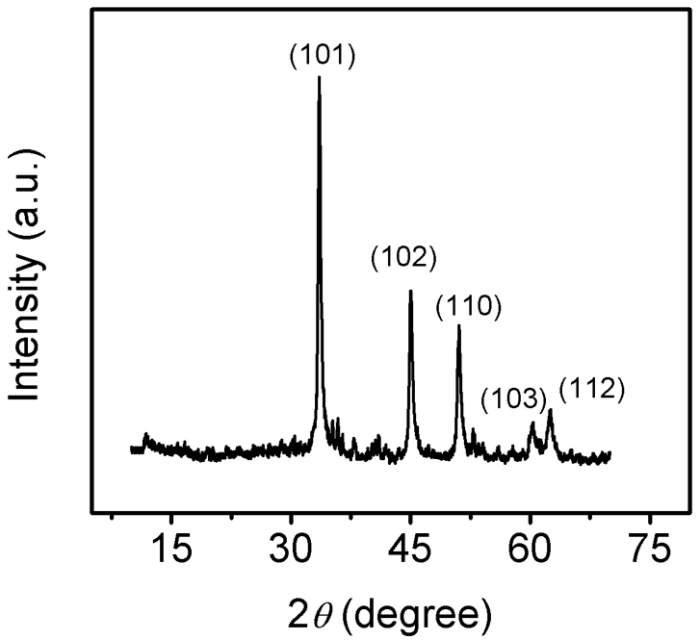

Figure 1. XRD pattern of the $Co_{0.85}Se$ sample.

The XRD pattern of the $Co_{0.85}Se$ powder sample is shown in Figure 1. All peak positions can be well indexed to $Co_{0.85}Se$ [JCPDS No. 52-1008]. No other peaks associated with impurities are

observed, which indicates the purity of the synthesized sample. The compositions of Co and Se were quantified by ICP-AES. The results show that the atomic ratio is 0.832:1.000 for Co:Se, which is close to the stoichiometric ratio of $Co_{0.85}Se$.

Common SEM images and corresponding EDS of the $Co_{0.85}Se$ and $Pt/Co_{0.85}Se$ on the surface of the GCE are shown in Figure 2. $Co_{0.85}Se$ exhibits a foliate structure, similar to the structure of graphene, which is consistent to a previous report (Figure 2A) [31]. The foliate structure of $Co_{0.85}Se$ produces a large surface area, which is beneficial to electrodeposition and electrocatalysis. When trace Pt was electrochemically reduced on $Co_{0.85}Se$ by CV, as shown in Figure 2B, the morphology of the $Co_{0.85}Se$ structure became more compact. However, we did not clearly find Pt NPs due to their low abundance on the surface of $Co_{0.85}Se$. Spectra of $Co_{0.85}Se$ from EDS analysis (Figure 2C) clearly showed the existence of elemental Co and Se in their stoichiometric ratio ($Co_{0.85}Se$). After being deposited on the $Co_{0.85}Se$/GCE by cyclic voltammetry (Figure 2D), Pt peaks appear and the O peak decreases, which indicates that trace Pt is reduced from H_6PtCl_6 on the surface of $Co_{0.85}Se$ and the oxygen-containing groups decrease with cyclic potential scanning. The amount of Pt on $Co_{0.85}Se$ was quantified by ICP-AES to be 22.65 μg cm^{-2}, which was calculated by the effective area of the $Pt/Co_{0.85}Se$ modified electrode.

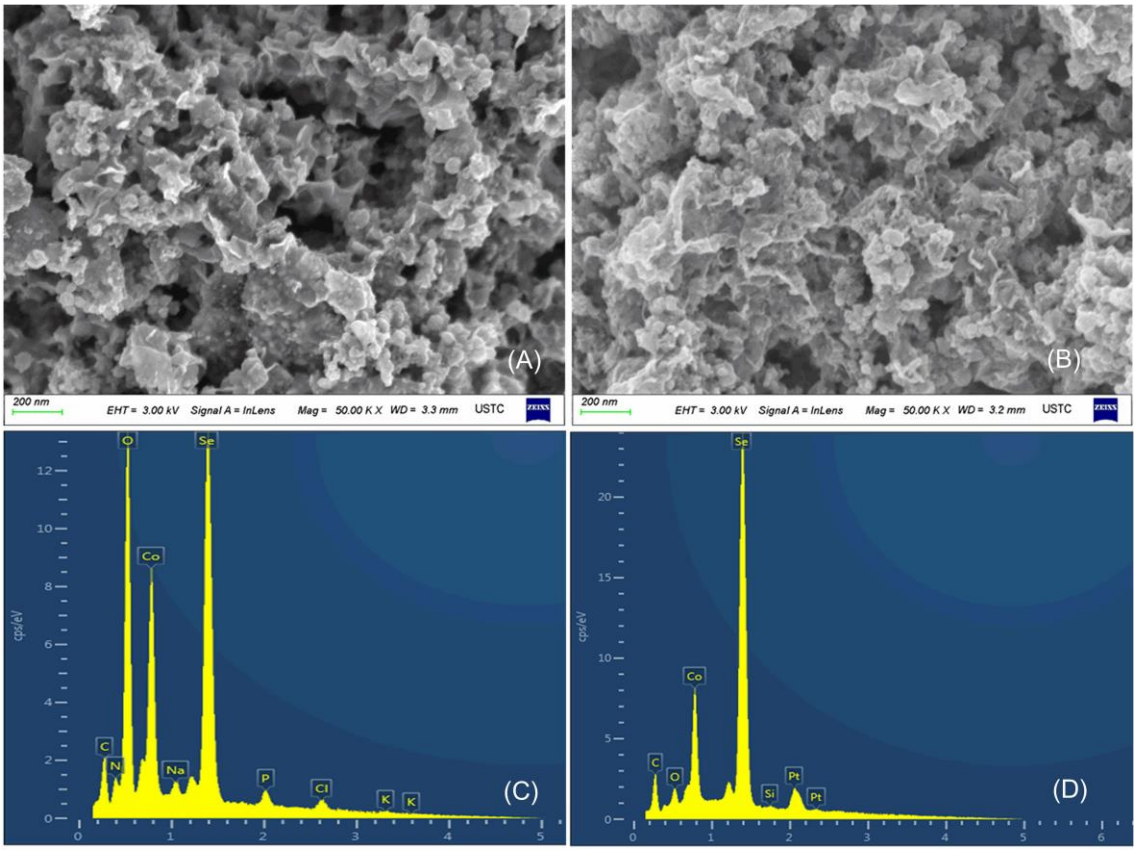

Figure 2. Common SEM images of $Co_{0.85}Se$ (A) and $Pt/Co_{0.85}Se$ (B) modified GCEs. EDS images of $Co_{0.85}Se$ (C) and $Pt/Co_{0.85}Se$ (D) modified GCEs.

3.2. Electrochemical behavior of the modified electrodes

Figure 3A presents the CVs of the different modified electrodes in 5.0 mM $K_3[Fe(CN)_6]$ at a scan rate of 0.05 V s^{-1}. As expected, quasi-reversible redox behaviors of $K_3[Fe(CN)_6]$ were observed on the bare GCE, Pt/GCE, $Co_{0.85}Se$/GCE, and Pt/$Co_{0.85}Se$/GCE with separations of cathodic and anodic peaks (ΔE_p) of 67, 75, 91 and 86 mV, respectively. The peak currents of Pt/GCE, $Co_{0.85}Se$/GCE, and Pt/$Co_{0.85}Se$/GCE increased and their ΔE_p were comparable to that of the bare GCE. The peak current on the Pt/$Co_{0.85}Se$/GCE increased by approximately 29% as compared to GCE, Pt/GCE, and $Co_{0.85}Se$/GCE. These electrochemical behaviors indicate that the Pt/$Co_{0.85}Se$ nanocomposites facilitate fast electron transfer between the probe and the electrode surface [32].

The microscopic electrochemically active area of Pt/$Co_{0.85}Se$/GCE was investigated by CV using $K_3[Fe(CN)_6]$ as the redox probe at different scan rates. The electrochemically active area (A) of the modified electrode can be calculated by the Randles-Sevcik equation: $i_{pa} = 2.69 \times 10^5 A D^{1/2} n^{3/2} v^{1/2} c$ [33,34], where i_{pa} is the anodic peak current, n is the electron transfer number, D is the diffusion coefficient of the probe, v is the scan rate, and c is the concentration of $K_3[Fe(CN)_6]$ probe. As shown in Figure 3B, the i_{pa} value increased linearly with the square root of scan rate (R=0.9976). This characteristic indicates that the electrochemical reaction of the redox probe on Pt/$Co_{0.85}Se$/GCE is a quasi-reversible and diffusion-controlled electrochemical process in this scan range [35]. For 5.0 mM $K_3[Fe(CN)_6]$ with 0.10 M KCl electrolyte, n=1, D= 6.70×10^{-6} cm^2 s^{-1} [36], the electrochemical active area of Pt/$Co_{0.85}Se$/GCE was calculated as 0.0989 cm^2 from the slope of the relationship between i_{pa} and $v^{1/2}$ (inset in Figure 3B), which indicates a larger surface area associated with Pt/$Co_{0.85}Se$/GCE compared to bare GCE (0.0706 cm^2) [37]. From all above results, it is clear that Pt/$Co_{0.85}Se$/GCE possesses larger specific surface area, higher electroactivity comparing to those of GCE, Pt/GCE, and $Co_{0.85}Se$/GCE.

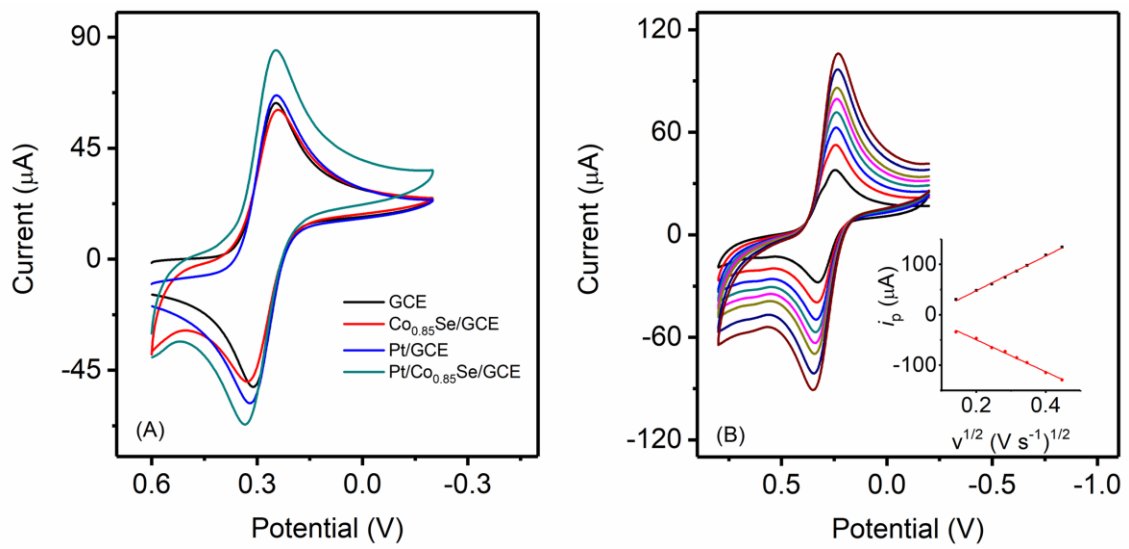

Figure 3. (A) CVs for bare GCE, $Co_{0.85}Se$/GCE, Pt/GCE, and Pt/$Co_{0.85}Se$/GCE in 5.0 mM $K_3[Fe(CN)_6]$ containing 0.10 M KCl. (B) CVs of the Pt/$Co_{0.85}Se$/GCE in 5.0 mM $K_3[Fe(CN)_6]$ at different scan rate of 0.02, 0.04, 0.06, 0.08, 0.1, 0.12, 0.16, and 0.2 V s^{-1} (from inner to outer lines).

3.3. Electrochemical catalysis and conditional optimization of the Pt/$Co_{0.85}$Se/GCE

AA DA, and UA probably coexist in biological samples and they show serious interference in the electrochemical determination DA [17]. Therefore, the electrochemical behaviors of the three species on the Pt/$Co_{0.85}$Se/GCE were investigated to evaluate the electrocatalytic activity and selectivity. Figure 4A displays DPVs for the electrochemical oxidation of a ternary mixture containing 0.59 mM AA, 5.96 μM DA, and 15 μM UA in 0.10 M PBS (pH 7.0) using different modified electrodes. Significantly, due to the synergistic effecst of the Pt and $Co_{0.85}$Se nanomaterials, not only the oxidation peaks of DA, AA, and UA separate from overlapped at bare GCE, Pt/GCE, or $Co_{0.85}$Se/GCE to distinguishable in turn at Pt/$Co_{0.85}$Se/GCE, but also the oxidation peak currents of the three biomolecules increased obviously. The peak separations between AA and DA, and between DA and UA are 136 mV and 131 mV, respectively, which are larger or comaprable to the reported results [1, 38]. It indicates that the Pt/$Co_{0.85}$Se/GCE has good distinguishing ability toward the catalytic oxidation of AA, DA, and UA and selective determination of DA can be achieved by the proposed sensor.

To achieve the best electrochemical response, effects of the electrolyte solution including the KCl concentration, Tris-HCl buffer (0.10 M, pH 8.1), acetate buffer (0.10 M, pH 5.0), sodium citrate buffer (0.10 M, pH 4.1), and the amounts $Co_{0.85}$Se were optimized. The present system, the solution of 0.10 M PBS with 0.10 M KCl (pH 7.0), showed good electrocatalysis and distinguishing ability toward AA, DA, and UA. For decreasing the usage of the noble metal Pt, only 4 μL 4.69 mM H_2PtCl_6 was dropped on the dried film of the 10 μL 1.44 mg mL^{-1} $Co_{0.85}$Se modified GCE, and was then electrochemically deposited to obtain Pt/$Co_{0.85}$Se/GCE, which exhibited excellent electron transfer between the electrode and the probe (Figure 3A)

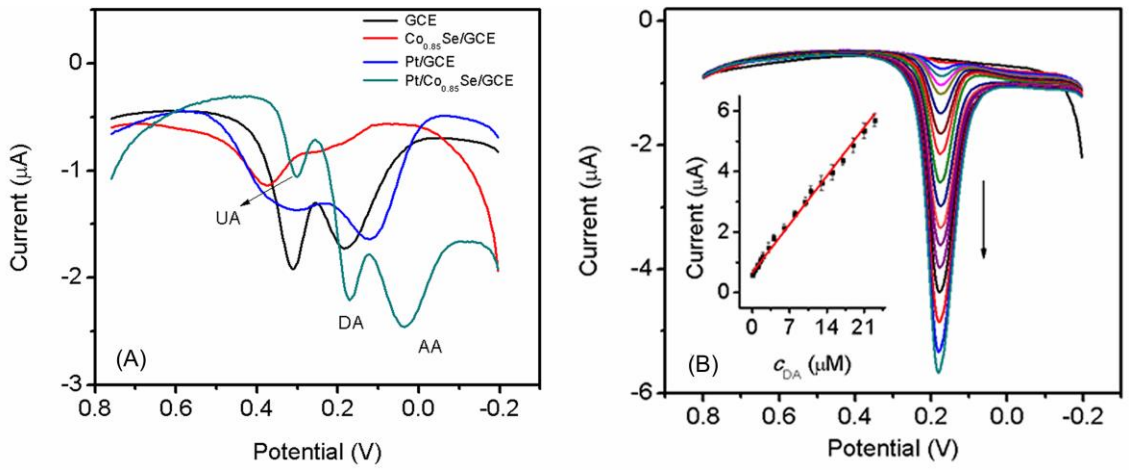

Figure 4. (A) DPVs at bare GCE, $Co_{0.85}$Se/GCE, Pt/GCE, and Pt/$Co_{0.85}$Se/GCE in 0.10 M PBS (pH 7.0) containing 0.59 mM AA, 5.96 μM DA, and 15 μM UA, respectively. (B) DPVs at Pt/$Co_{0.85}$Se/GCE in 0.10 M PBS containing different concentrations of DA (0.50–22.0 μM).

Figure 4B displays the DPVs used for the determination of DA on Pt/$Co_{0.85}$Se/GCE. With successive additions of DA, the DPV oxidation peak currents increased linearly as the concentration increased, and the oxidation potentials remained unchanged at a high concentration. The corresponding

linear responses for the determination of DA were obtained in concentration ranges of 0.50–22.0 μM (R=0.992) with a limit of detection (LOD) of 0.39 μM. The response sensitivity for DA was 2306 μA mM cm^{-2}. Compared to other nanomaterial modified sensors (Table 1), the Pt/$Co_{0.85}$Se/GCE exhibited wide linear ranges, high response sensitivity, and a low LOD. The results suggest that Pt/$Co_{0.85}$Se is a novel potential material for the fabrication of nonenzymatic electrochemical sensors.

Table 1. Comparison of the response characteristics of different sensors for DA determination

Electrode	Linear range (μM)	LODs (μM)	Sensitivity (μA mM^{-1} cm^{-2})	Ref.
PImox–GO/GCE [a]	12–278	0.63	1953	[39]
Graphene-AT /GCE	5–25	5	27200	[40]
GO-PAN/GCE	1–14	0.5	–	[41]
RGO/AuNPs	1.0–100	0.69	2231	[42]
PG/GCE	5.00–710	2.00	568	[43]
GEF/CFE	0.7–45.21	0.5	–	[44]
Pt/GCE	0.03–8.1	0.03	–	[45]
Nafion/Pt/MC/GCE	0.50–23.0	0.39	2306	This work

a. Abbreviations: PImox: polyimidazole; GO: graphene oxide; AT: 2-Amino-thiazol; PAN: polyaniline; RGO: reduced graphene oxide; PG: pristine graphene. GEF: Graphene flowers; CFE: carbon fiber electrode.

3.4. Properties and application of the presented sensor

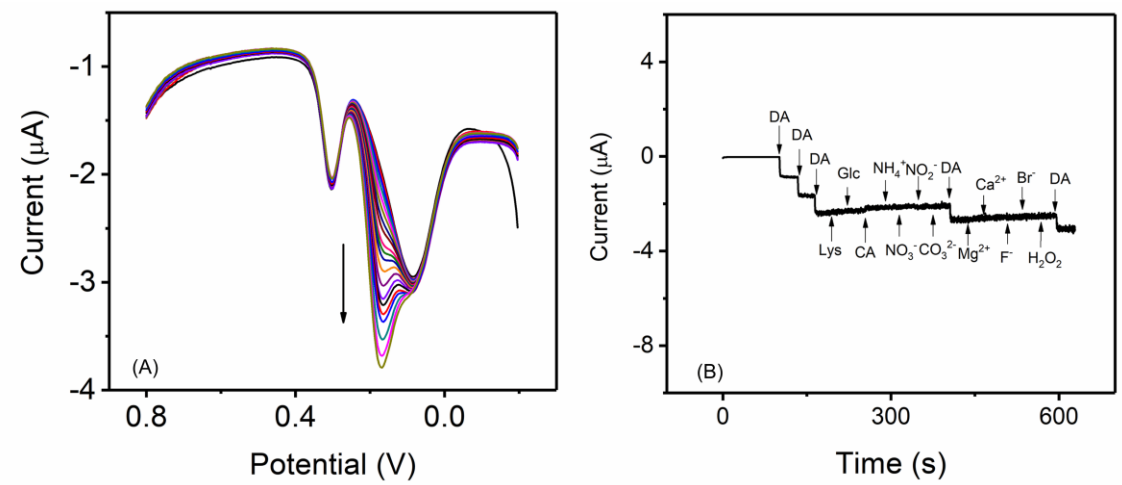

Figure 5. (A) DPVs at Pt/$Co_{0.85}$Se/GCE in 0.10 M PBS (pH 7.0) containing 0.25 mM AA, 56 μM UA, and various concentrations of DA. (B) Amperometric responses of the sensor with three additions 66.7 μM DA and successive additions 0.83 mM Lys, Glc CA, 1.7 mM NH_4^+, NO_3^-, CO_3^{2-}, NO_2^-, Mg^{2+}, Ca^{2+}, F^-, Br^-, and 0.2 mM H_2O_2.

In addition to sensitivity, high selectivity is a crucial parameter in real sensors for detecting DA. To evaluate the ability of anti-interference, the ternary mixture containing AA, DA, and UA was investigated. In the ternary mixture, the concentration of DA changed, whereas those of AA and UA

remained constant. As shown in Figure 5A, the peak current of DA increases with the addition of DA while the peak currents of AA and UA do not change obviously. The results indicate that the proposed sensor exhibits good selectivity in the ternary mixture.

Furthermore, the influences of potential interferences including lysine (Lys), glucose (Glc), citric acid (CA), NH_4^+, NO_3^-, CO_3^{2-}, NO_2^-, Mg^{2+}, Ca^{2+}, F^-, Br^-, and H_2O_2 were investigated by the amperometric current-time method. As shown in Figure 5B, the Pt/$Co_{0.85}$Se/GCE responds quickly to the oxidation of 66.7 μM DA and achieves a steady-state current within 1.6 s after addition of DA. However, no noteworthy current responses were observed for the additions of 0.83 mM Lys, Glc, CA, 1.7 mM NH_4^+, NO_3^-, CO_3^{2-}, NO_2^-, Mg^{2+}, Ca^{2+}, F^-, Br^-, and 0.2 mM H_2O_2, which suggests that the presence of these substances does not interfere with the detection of DA.

The stability of the sensor was evaluated by successive sensor responses to DA for 1 h. As shown in Figure 6, the catalytic current is very stable and only shows a slight decay after 1 h of successive detection (Figure 6). Moreover, the catalytic current still exhibits sensitive response to DA after 1 h, indicating its excellent operational stability. The long-term stability was also investigated by the current response to DA. After 20 day of storage, the presented sensor retained 99.3% of its original current response to DA. The results confirm the excellent operational and storage stability of the sensor.

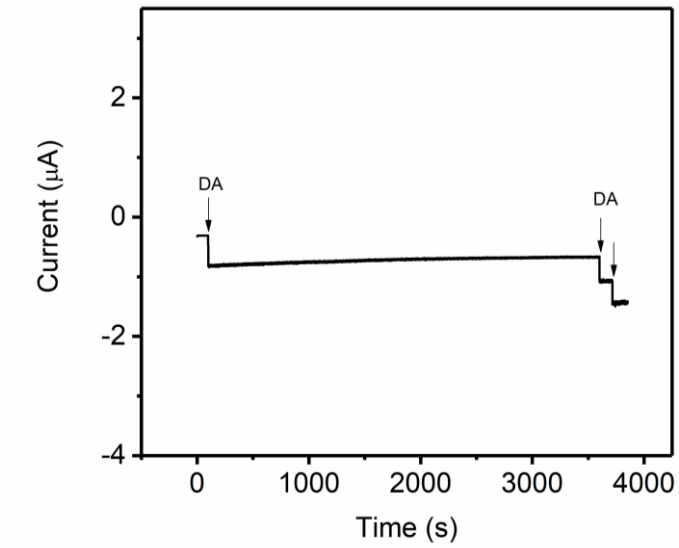

Figure 6. Successive current response of the sensor to 33 μM DA before and after the 1 h response.

In addition, the intra- and inter-reproducibility of the sensor were evaluated by 5 different prepared sensors on a single GCE and 5 sensors with five different GCEs, respectively. The modified proccess was treated by the same method. The relative standard deviations (RSD) are both less than 4.8% for the intra- and inter-reproducibility. The results indicate acceptable reproducibility of the presented sensor.

The utilization of the proposed sensor in a serum sample was studied by using the standard addition method. Prior to the measurements, the serum sample was centrifuged at 4000 rpm at 4 °C for 20 min, and was then diluted 1:20 with 0.10 M PBS. According to the standard curves that are shown

in Figure 4, the recoveries for the determination of DA range between 97% and 106% (Table 2), which reveal that the fabricated sensor based on Pt/$Co_{0.85}Se$ nanomaterials can be practically applied in biological samples.

Table 2. Determination of DA in real samples

Sample	Detected (μM)	Added (μM)	Total (μM)	Recovery (%)
1	0.51	2.0	2.64	106
2	0.49	4.0	4.62	103
3	0.53	8.0	8.29	97

4. CONCLUSIONS

An interfacial material was proposed via combination of $Co_{0.85}Se$ and trace Pt (Pt/$Co_{0.85}Se$), which was first used to fabricate a novel nonenzymatic electrochemical sensor (Pt/$Co_{0.85}Se$/GCE). The modified interface has a large effective surface area and fast electron-transfer kinetics due to synergistic effects of the catalytic activity of platinum, the foliate structure, and conductivity of $Co_{0.85}Se$. The prepared sensor exhibits high sensitivity and good distinguishing ability towards the oxidation of AA, DA, and UA. Moreover, the sensor shows excellent response stability and reproducibility for the determination of DA with a wide linear range and a low LOD.

ACKNOWLEDGEMENTS
This work was supported by the National Natural Science Foundation of China (21405019, 91643113, 21637004), the Cooperative Project between Fuyang Municipal Government and Fuyang Normal University (XDHX201701, XDHX201704), the Natural Science Foundation of Anhui Province (1708085MB43), the Key Projects of the Support Program for Outstanding Young Talents in Anhui Province Colleges and Universities (gxyqZD2016192, gxyqZD2016193), the Natural Science Foundation of Higher Education Institutions in Anhui Province (KJ2018ZD035), the Anhui Provincial Teaching Team program (2017jxtd025), Quality project of higher education of Anhui Province (2016jyxm0749).

References

1. S.H. Zhou, H.Y. Shi, X. Feng, K.W. Xue, W.B. Song, *Biosens. Bioelectron.*, 42 (2013) 163–169.
2. H. Li, Y. Wang, D. Ye, J. Luo, B. Su, S. Zhang, J. Kong, *Talanta*, 127 (2014) 255–261.
3. N. González-Diéguez, A. Colina, J. López-Palacios, A. Heras, *Anal. Chem*., 84 (2012) 9146–9453.
4. X.Q. Ouyang, L.Q. Luo, Y.P. Ding, B.D. Liu, D. Xu, A.Q. Huang, *J. Electroanal. Chem*., 748 (2015) 1–7.
5. L. Wang, M. Asgharnejad, *J. Pharmaceut. Biomed*., 21 (2000) 1243–1248.
6. Q.C. Mo, F. Liu, G. Jing, M.P. Zhao, N. Shao, *Anal. Chim. Acta*, 1003 (2018) 49–55.
7. V. Gökmen, N. Kahraman, N. Demir, J. Acar, *J. Chromatogr*. A, 81 (2000) 309–316.
8. N. Xia, L. Liu, R. Wu, H. Liu, S.J. Li, Y. Hao, *J Electroanal. Chem*., 731 (2014) 78–83.
9. J.J. Jiang, X.Z. Du, *Nanoscale*, 6 (2014) 11303–11309.
10. X.F. Liu, L. Zhang, S.P. Wei, S.H. Chen, X. Ou, Q.Y. Lu, *Biosens. Bioelectron*., 57 (2014) 232–238.

11. S.C. Hsu, H.T. Cheng, P.X. Wu, C.J. Weng, K.S. Santiago, J.M. Yeh, *Electrochim. Acta*, 238 (2017) 246–256.
12. B.R. Wang, J.C. He, F.Q. Liu, L. Ding, *J. Alloy Compd*., 693 (2017) 902–908.
13. H. Wu, S. Fan, X. Jin, H. Zhang, H. Chen, Z. Dai, X. Zou, *Anal. Chem*., 86 (2014) 6285–6290.
14. H. Wu, X. Li, M. Chen, C. Wang, T. Wei, H. Zhang, S. Fan, *Electrochim. Acta*, 259 (2018) 355–364.
15. S. Fan, Y. Zhu, R. Liu, H. Zhang, Z. Wang, H. Wu, *Sens. Actuators* B.,2016, 233, 206–213.
16. C. Su, C. Sun, Y. Liao, ACS Omega, 2 (2017) 4245−4252.
17. A. Puangjan, S. Chaiyasith, W. Taweeporngitgul, J. Keawtep, *Mat. Sci. Eng. C-Mater*., 76 (2017) 383–397
18. A. Vlandas, T. Kurkina, A. Ahmad, K. Kern, K. Balasubramanian, *Anal. Chem*., 82 (2010) 6090−6097.
19. Y.G. Lee, B.X. Liao, Y.C. Weng, *Chemosphere*, 173 (2017) 512−519.
20. Q. Feng, X. Zhao, Y. Guo, M. Liu, P. Wang, *Biosens. Bioelectron*., 108 (2018) 97−102.
21. M.A. Raj, S.A. John, *J. Phys. Chem*. C, 117 (2013) 4326−4335.
22. S. Thiagarajan, S.M. Chen, *Talanta*, 74 (2007) 212–222.
23. C.L. Sun, H.H. Lee, J.M. Yang, C.C. Wu, *Biosens. Bioelectron*., 26 (2011) 3450−3455.
24. Z. Dursun, B. Gelmez, *Electroanal.*, 22 (2010) 1106−1114.
25. B. Singh, F. Laffir, T. McCormac, E. Dempsey, *Sens. Actuators* B., 150 (2010) 80–92.
26. S. Zhou, Q. Jiang, J. Yang, W. Chu, W. Li, X. Li, Y. Hou, J. Hou, *Electrochim. Acta*, 220 (2016) 169–175.
27. Y. Zhang, A. Pan, L. Ding, Z. Zhou, Y. Wang, S. Niu, S. Liang, G. Cao, *ACS Appl. Mater. Interfaces*, 9 (2017) 3624−3633.
28. H. Peng, G. Ma, K. Sun, Z. Zhang, J. Li, X. Zhou, Z. Lei, *J. Power Sources*, 297 (2015) 351–358.
29. J. Dong, J. Wu, J. Jia, S. Wu, P. Zhou, Y. Tu, Z. Lan, *Electrochim. Acta*, 168 (2015) 69–75.
30. S. Li, S. Peng, L. Huang, X. Cui, A.M. Al-Enizi, G. Zheng, *ACS Appl. Mater. Interfaces*, 8 (2016) 20534−20539.
31. F. Gong, H. Wang, X. Xu, G. Zhou, Z.-S. Wang, *J. Am. Chem. Soc*., 134 (2012) 10953−10958.
32. A.T. E. Viliana, S.-M. Chen, L.-H. Huang, M. Ajmal Ali, F.M.A. Al-Hemaid, *Electrochim. Acta*, 125 (2014) 503–509.
33. J.R. Miller, J.A. Taies, J. Silver, *Inorg. Chim. Acta*, 138 (1987) 205−214.
34. Q. Ma, S. Ai, H. Yin, Q. Chen, T. Tang, *Electrochim. Acta*, 55 (2010) 6687–6694.
35. A. Puangjan, S. Chaiyasith, W. Taweeporngitgul, J. Keawtep, *Mat. Sci. Eng. C*, 76 (2017) 383 –397.
36. J. Sun, L. Li, X. Zhang, D. Liu, S. LV, D. Zhu, T. Wu, T. You, *RSC Adv.*, 5 (2015) 11925–11932.
37. L. Fotouhi, M. Fatollahzadeh, M. M. Heravi, *Int. J. Electrochem. Sci.*, 7 (2012) 3919–3928.
38. S. Wu, L. Xiao, Z. Du, H. Wang, Q. Yuan, H. Ji, *J. Electroanal. Chem.*, 804 (2017) 72–77.
39. X. Liu, L. Zhang, S. Wei, S. Chen, X. Ou, Q. Lu, *Biosens. Bioelectron*., 57 (2014) 232–238.
40. T.H. Tsai, Y.C. Huang, S.M. Chen, M.A. Ali, F.M.A. AlHemaid, *Int. J. Electrochem. Sci*., 6 (2011) 6456−6468.
41. Y. Bao, J. Song, Y. Mao, D. Han, F. Yang, L. Niu, and A. Ivaska, *Electroanal*., 23 (2011) 878–884.
42. C.S. Lee, S.H. Yu, T.H. Kim, *Nanomaterials*, 8 (2018) 17.
43. S. Qi, B. Zhao, H. Tang, X. Jiang, *Electrochim. Acta*, 161 (2015) 395–402.
44. J. Du, R.R. Yue, F.F. Ren, Z.Q. Yao, F.X. Jiang, P. Yang, Y.K. Du, *Biosens. Bioelectron*., 53 (2014) 220−224.
45. C.L. Sun, H.H. Lee, J.M. Yang, C.C. Wu, *Biosens. Bioelectron*., 26 (2011) 3450−3455.